[CANCER RESEARCH 61, 439–444, January 15, 2001]

Advances in Brief

A Novel Response of Cancer Cells to Radiation Involves Autophagy and Formation of Acidic Vesicles[1]

Shoshana Paglin, Timothy Hollister, Thomas Delohery, Nadia Hackett, Melissa McMahill, Eleana Sphicas, Diane Domingo, and Joachim Yahalom[2]

Department of Radiation Oncology [S. P., T. H., N. H., M. M., J. Y.], and Flow Cytometry Core Facility [T. D., D. D.], Memorial Sloan-Kettering Cancer Center, New York, New York 10021, and the Electron Microscopy Service, Rockefeller University, New York, New York 10021 [E. S.]

Abstract

The mechanisms underlying neoplastic epithelial cell killing by ionizing radiation are largely unknown. We discovered a novel response to radiation manifested by autophagy and the development of acidic vesicular organelles (AVO). Acidification of AVO was mediated by the vacuolar H^+-ATPase. Staining with the lysosomotropic agent acridine orange enabled us to quantify AVO accumulation and to demonstrate their time- and dose-dependent appearance. The appearance of AVO occurred in the presence of the pan-caspase inhibitor z-Val-Ala-Asp(Ome)-fluoromethyl ketone, but was inhibited by 3-methyladenine, an inhibitor of autophagy. The accretion of AVO in surviving progenies of irradiated cells, and the increased incidence of clonogenic death after inhibition of vacuolar H^+-ATPase suggest that formation of acidic organelles represents a novel defense mechanism against radiation damage.

Introduction

The cellular and molecular processes involved in the response of neoplastic epithelial cells to radiation are largely unknown. Whereas in some cell types, particularly cells of reticuloendothelial origin, death after irradiation is preceded by apoptotic changes, apoptosis plays little or no role in the killing of epithelial neoplastic cells by radiation (1–3). Epithelial cells do not undergo apoptosis after irradiation and are likely to respond with a different sequence of programmed cytoplasmic and nuclear events. Several investigators have proposed two types of programmed cell death (4, 5). Type I programmed cell death, or apoptosis, is mediated by a cascade of cysteine aspartases (caspases) and factors released by the mitochondria (6), and it has typical morphological and biochemical characteristics such as chromatin margination and condensation, early nuclear collapse, and nucleosomal ladder formation (5). In contrast, type II programmed cell death is marked morphologically by increased autophagy and early destruction of the cytoplasm that occurs either without nuclear collapse or precedes it (5). Type II programmed cell death has been documented mainly in the *Lepidoptera* during metamorphosis and during involution of the rat mammary gland (4, 5), but it has rarely been associated with stress-inducing stimuli (7, 8). Unfortunately, methods for quantification of type II programmed cell death are lacking, and the molecular mechanisms that regulate it have not been defined. The work presented here characterizes and quantifies a novel form of response to radiation in cancer cells that is reminiscent of type II programmed cell death. This response is dominated by the appearance and accumulation of AVO.[3] Interference with the acidification of these AVO results in increased radiosensitivity and thus identifies a new target for modulating the radiation response of cancer cells.

Materials and Methods

Cell Culture. MCF-7 (human breast adenocarcinoma), LoVo (human colon adenocarcinoma), and LNCaP (human prostate carcinoma) were obtained from the American Type Culture Collection. Cells were maintained as described previously (9). Irradiation was carried out 48 h post-plating (time 0) at 25°C using a Cs-137 irradiator (Shepherd Mark-I, model 68, SN643) at a dose-rate of 243 cGy/min. Bovine aortic endothelial cells were obtained from Dr. Haimovitz-Friedman, Memorial Sloan Kettering Cancer Center, New York) and were grown and treated with H_2O_2 as described previously (10, 11). PMA (Alexis Biochemicals Corporation, San Diego, CA) was dissolved in DMSO and added to cells for the duration of 1 h. Final DMSO concentration was 0.03%. The cells were then rinsed with warm growth medium before being returned to the incubator for an additional 48 h.

Supravital Cell-staining with Acridine Orange. Cell staining was performed according to published procedures (12–14). Acridine orange (Polysciences, Warrington, PA) was added at a final concentration of 1 μg/ml for a period of 15 min. Bafilomycin A1 (Sigma Chemical Co., St. Louis, MO) was dissolved in DMSO and added to the cells 30 min before addition of acridine orange. LysoSensor Blue DND-167 (Molecular Probes, Eugene, OR) was added for 8 min at a final concentration of 10 μM. Pictures were obtained with a fluorescence microscope (Olympus BH-2 RFCA) equipped with a mercury 100-W lamp, 490-nm band-pass blue excitation filters, a 500-nm dichroic mirror, and a 515-nm-long pass-barrier filter. Images of control and irradiated cells were recorded on Kodak Elite II 100 ASA film for color slides by 4-s exposure.

Determination of Mean Red:Green Fluorescence Ratio in Acridine Orange-stained Cells Using Flow Cytometry. In acridine orange-stained cells, the cytoplasm and nucleolus fluoresce bright green and dim red, whereas acidic compartments fluoresce bright red (13, 14). The intensity of the red fluorescence is proportional to the degree of acidity and/or the volume of the cellular acidic compartment (14). Therefore, by comparing the mean red:green fluorescence ratio within different cell populations, we could measure a change in the degree of acidity and/or the fractional volume of their cellular acidic compartment. Cells were stained with acridine orange for 17 min, removed from the plate with trypsin-EDTA, and collected in phenol red-free growth medium. Green (510–530 nm) and red (>650 nm) fluorescence emission from 10^4 cells illuminated with blue (488 nm) excitation light was measured with a FACSCalibur from Becton Dickinson (San Jose, CA) using CellQuest software. The red:green fluorescence ratio for individual cells was calculated using FlowJo software (TREE STAR, Inc., San Carlos, CA). To control for the possible effect of trypsinization on the measured red:green fluorescence ratio, we compared the ratios obtained by flow cytometry with those obtained with a Laser Scanning Microscope (LSM510; Zeiss). Stained cells, grown on coverglass, were illuminated with a 488-nm argon laser beam. The red (>650 nm):green (505–545 nm) fluorescence ratio of an entire image was obtained

Received 4/25/00; accepted 11/20/00.

The costs of publication of this article were defrayed in part by the payment of page charges. This article must therefore be hereby marked *advertisement* in accordance with 18 U.S.C. Section 1734 solely to indicate this fact.

[1] Supported by grants from the Dewitt-Wallace Fund, the Sports Foundation Against Cancer, the Connecticut Sports Foundation, the Reich-Jossem Fund, and a Radiological Society of North America grant (to T. H.).

[2] To whom requests for reprints should be addressed, at Department of Radiation Oncology, Box 22, Memorial Sloan-Kettering Cancer Center, 1275 York Avenue, New York, NY 10021. Phone: (212) 639 5999; Fax: (212) 639 7742; E-mail: yahalomj@mskcc.org.

[3] The abbreviations used are: AVO, acidic vesicular organelles; PMA, phorbol 12-myristate 13-acetate; LAMP, lysosome-associated membrane protein; DAMP, {N-[3-(2,4-dinitrophenyl)-N-(3-aminopropyl)]methylamine dihydrochloride}; TUNEL, terminal deoxynucleotidyl transferase-mediated nick end labeling.

using software LSM 510 version 2.01 SP2. These measurements yielded similar results to those obtained with flow cytometry. All determinations of red:green fluorescence ratio reported here were therefore obtained via flow cytometry.

Electron Microscopy. Cell processing for electron microscopy and staining with DAMP (Molecular Probes, Eugene, OR) was done according to published procedures (15, 16). The fraction of the cytoplasmic volume occupied by AVO (the fractional volume of AVO) was quantified from electron micrographs according to Dunn (16) and Lenk *et al.* (17). Digital images of the micrographs were obtained with an Epson ES-1200S flat bed scanner with Adobe Photoshop version 5. The fractional volume was calculated with Image Pro Plus version 3 and expressed as a percentage of total cytoplasmic volume.

Detection of Nucleosomal Fragmentation of Genomic DNA. DNA extraction and electrophoresis on agarose gel was carried out according to Bose *et al.* (18). DNA preparation and resolution with pulse field gel electrophoresis was conducted as described by Gilles *et al.* (19) using the CHEF Mapper (Bio-Rad, Richmond, CA). DNA strand breaks were assayed by the TUNEL method and analyzed by flow cytometry (10).

Gel Electrophoresis and Western Blotting. Cells were scraped and collected in PBS containing protease inhibitors (Complete and pepstatin A; Boehringer Mannheim) and lysed in 2% SDS by heating at 95°C. Protein content was determined with bicinchoninic acid reagent (Pierce). PAGE and immunoblotting were performed (20) using anti-LAMP-1 antibodies (Hybridoma Bank, Department of Biological Sciences, Iowa City, IA).

Immunocytochemistry. Cells were fixed with 3% paraformaldehyde, permeabilized with 1% Triton X-100, and stained with anti-LAMP-1 and Texas Red conjugated antimouse IgG (Jackson ImmunoResearch Laboratories, Inc., Jackson, Il).

Surviving Fraction. Cells were plated in growth medium at a density of 30 cells/cm^2 and irradiated 22 h later with 2 and 3 Gy. Cells were irradiated at room temperature in a Cs-137 Irradiator (Sheperd Mark-I, Model 68, SN 643) at a rate of 2.5 Gy/min. Six days later, 90–95% of the grown colonies possessed >50 cells. For determination of their red:green ratio, colonies were processed as described above. For determination of surviving fractions, cells were stained with crystal violet and colonies containing ≥50 cells were counted with a dissecting microscope. The surviving fraction was defined as the ratio between the number of surviving colonies in irradiated culture and in unirradiated culture, and it was calculated at each dose level (21).

Results and Discussion

Our experiments indicated that human breast cancer cells are sensitive to standard doses of radiation. After irradiation with 6 Gy, only 0.1% of the cells remained clonogenic (22). Nonetheless, the cells did not show any of the biochemical and morphological changes that are associated with apoptosis up to 4 days after irradiation with 10 Gy. At 4 days after irradiation, 30% of the cells were already dead and did not exclude trypan blue. Still, nucleosomal ladder formation and a positive TUNEL reaction could not be demonstrated (Fig. 1). Furthermore, electron microscopy did not reveal the morphological changes that are typical of apoptosis, *i.e.*, chromatin margination and condensation (Fig. 2). Instead, DNA damage was manifested by micronuclei formation (9) and nondiscrete DNA degradation (Fig. 1). Our findings and the absence of apoptotic markers after irradiation of malignant epithelial cells reported by others (1, 2) led us to search for type II programmed cell death-related cellular events, such as changes in the cellular acidic compartments.

For detecting of the acidic compartment, we used the lysosomotropic agent acridine orange, a weak base that moves freely across biological membranes when uncharged. Its protonated form accumulates in acidic compartments, where it forms aggregates that fluoresce bright red (12–14). Vital staining of MCF-7 cells with acridine orange revealed the appearance of AVO after irradiation. Concentrated dye in the vesicles fluoresced bright red, whereas the cytoplasm and the nucleus showed dominant green fluorescence (Fig. 3Ab). In contrast, the majority of unirradiated cells exhibited mainly green fluorescence with minimal red fluorescence (Fig. 3*Aa*). In numerous studies, demonstration of vacuolar H^+-ATPase-dependent acidification of cellular organelles, as well as its involvement in different cellular processes, was achieved by using its specific inhibitor bafilomycin A1 (23, 24). Similarly, by addition of the inhibitor to MCF-7 cells, we were able to demonstrate that acidification of AVO is mediated by the vacuolar H^+-ATPase (Fig. 3*A*, *b* and *c*; Ref. 23). Preincubation of the cells with 300 μM of the weak amine chloroquine also inhibited acridine orange accumulation in AVO (data not shown).

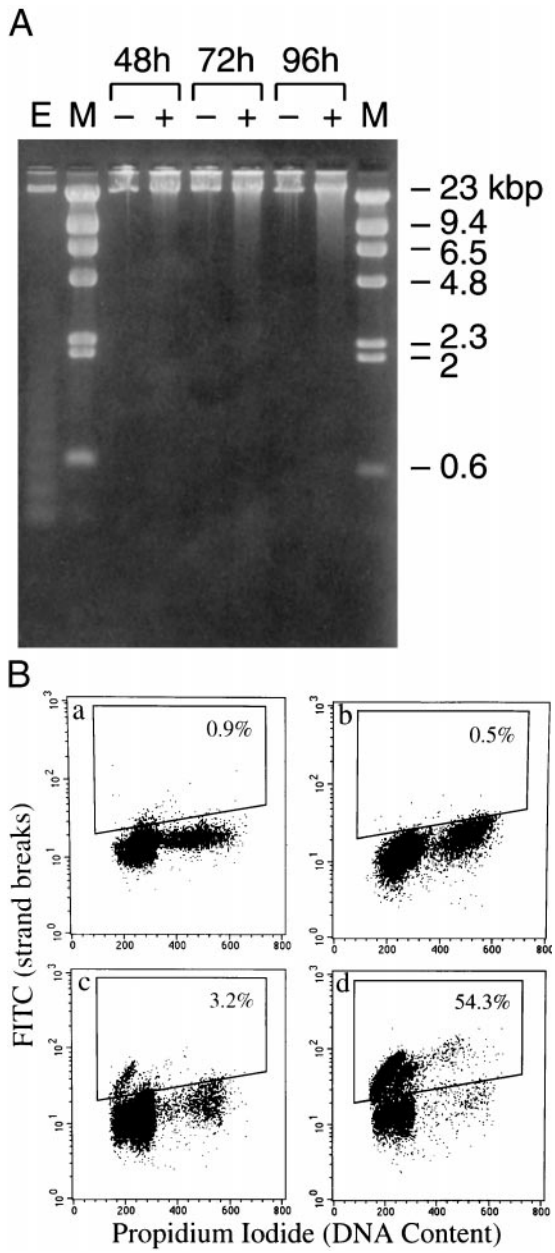

Fig. 1. Biochemical apoptotic hallmarks were not detected in irradiated MCF-7 cells. *A*, irradiated cells showing nondiscrete DNA degradation (+), and control unirradiated (−) cells were harvested at the noted time post-time 0 (irradiation time). Treatment of bovine aortic endothelial cells with H_2O_2, DNA extraction, and electrophoresis on agarose DNA gel were carried out as described in "Materials and Methods." *E*, endothelial cells; *M*, λ DNA/*Hin*dIII markers. *B*, MCF-7 and endothelial cells were treated as above and processed for the TUNEL procedure 48 h after irradiation. *a*, control MCF-7; *b*, irradiated MCF-7; *c*, untreated endothelial cells; *d*, H_2O_2-treated endothelial cells.

To measure the radiation-induced increase in fractional volume and/or acidity of AVO, we determined the mean red:green fluorescence ratio in control and irradiated cells. At 24 h after irradiation, 92% of the unirradiated controls were tightly distributed around their

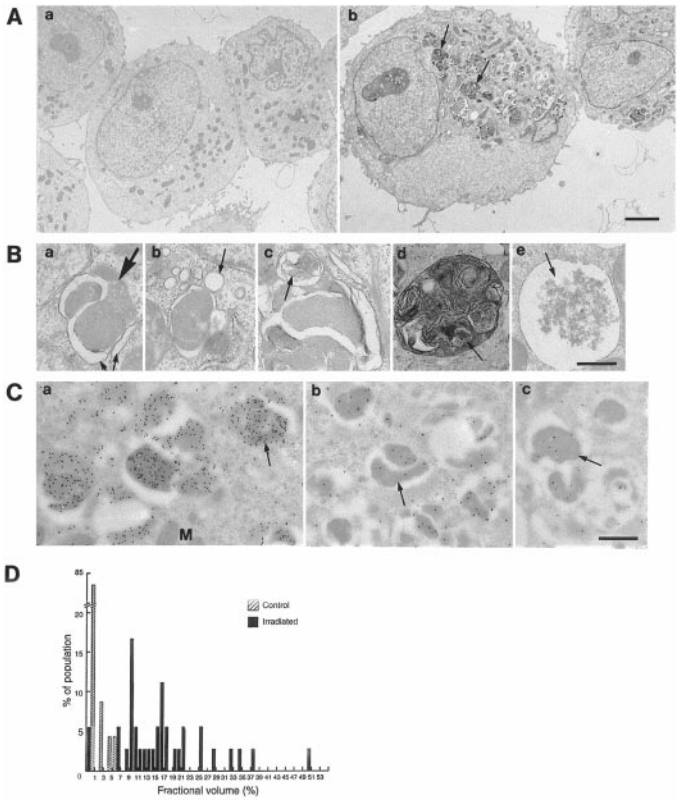

Fig. 2. Ultrastructure of AVO formed in irradiated cells. *A*, *a*, control unirradiated cells 48 h postirradiation time (Time 0). *b*, cells irradiated with 10 Gy, 48 h postirradiation. The *arrow* points to newly formed AVO. *Bar* (*a–b*), 4 μm. *B*, *a–e*, newly formed vesicular organelles in cells irradiated as above. The *arrows* point to the part-rough, part-smooth membrane cisternae (*a*), to vesicles fusing with membrane cisternae (*b*), to lamellar structures (*c* and *d*), and to residual digested material (*e*). *Bar* (*a–e*), 0.6 μm. *C*, concentration of the lysosomotropic agent DAMP in AVO (AVO-EM) demonstrated by immunogold histochemistry. Cells were stained with DAMP 24 h postirradiation with 10 Gy and processed for viewing as described in "Materials and Methods." The *arrow* points to the gold particles over the AVO (*a*). Cells were incubated with 0.5 μM bafilomycin A1 (*b*) or with 300 μM chloroquine (*c*) before the addition of DAMP. *Bar* (*a–c*), 0.6 μm. *D*, distribution of unirradiated and irradiated cell populations according to the fraction of the cytoplasmic volume occupied by AVO-EM (fractional volume). Fractional volume of AVO-EM was calculated as described in "Materials and Methods."

mean red:green fluorescence ratio (Fig. 3*Ba*). Only 8% had a red:green fluorescence ratio that increased asymptotically above 2 (the highest value in the descending limb of the histogram). On the other hand, 55% of the irradiated cells had a red:green ratio that was >2, and the mean value of red:green fluorescence ratio was 2.3-fold higher than in controls (Fig. 3*Bb*). Bafilomycin A1 decreased the mean red:green fluorescence ratio in unirradiated cells and also inhibited its radiation-induced increase. In the presence of bafilomycin A1, the mean red:green fluorescence ratio was similar in both unirradiated and irradiated cells, indicating that the radiation-induced increase in this ratio is attributable to the development of AVO, rather than other possible changes in the molecular composition of the irradiated cells (Fig. 3*B*, *c* and *d*). AVO appearance was dependent upon the radiation dose and increased with the time after irradiation (Fig. 4).

To differentiate further between the acidic compartments of control and irradiated cells, we used an additional lysosomotropic agent, LysoSensor Blue DND-167. The fluorescence of LysoSensor Blue is pH-dependent and increases as pH decreases. In unirradiated cells, LysoSensor Blue hardly showed any fluorescence, whereas irradiated cells fluoresced bright blue (Fig. 3*A*, *e* and *f*), indicating that the pH of the acidic compartments in irradiated cells is indeed lower than that of unirradiated cells. AVO appearance was associated with increased levels of the lysosomal membrane protein LAMP-1, as evident from Western blot analysis and immunocytochemistry (Fig. 5*A* and *B*).

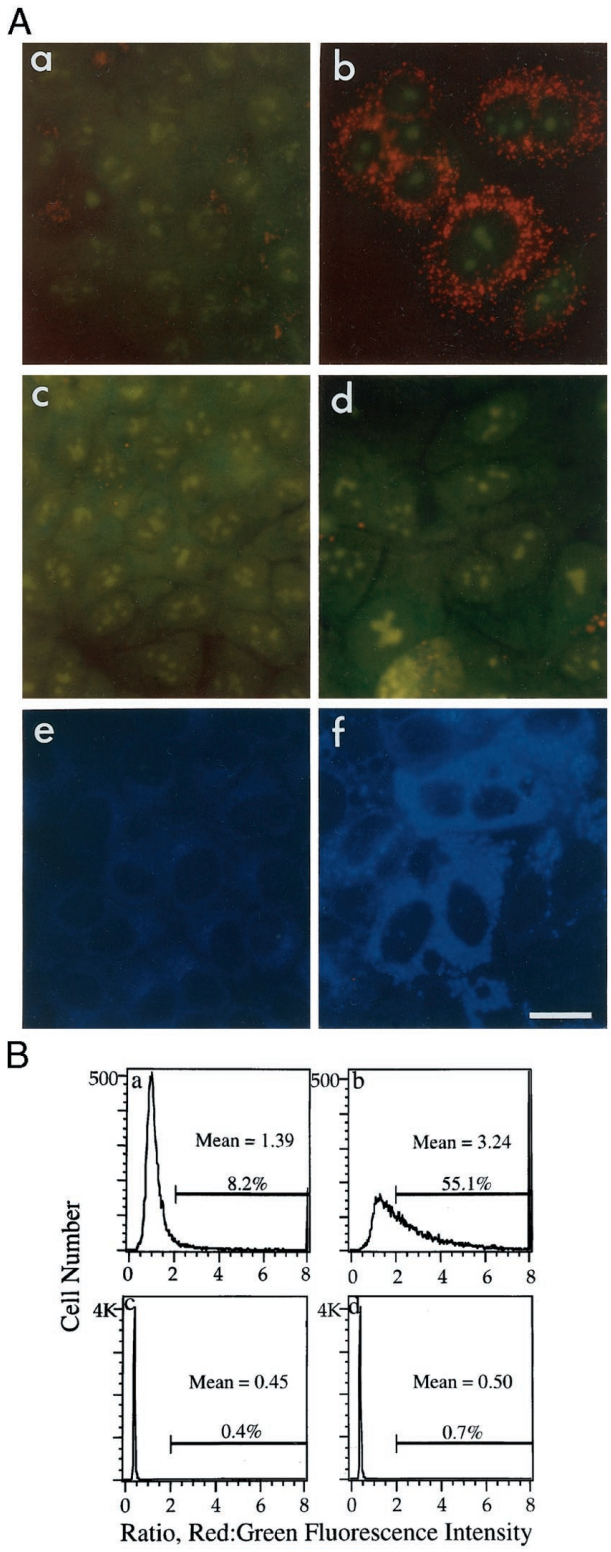

Fig. 3. *A*, detection of radiation-induced appearance of AVO by vital staining with lysosomotropic agents. Acridine orange: *a* and *c*, unirradiated cells; *b* and *d*, 30 h after irradiation with 10 Gy. *c* and *d*, cells were incubated with 200 nM bafilomycin A1 for 30 min before the addition of acridine orange. LysoSensor Blue DND-167: e, unirradiated cells; *f*, cells 30 h after exposure to 10 Gy. *Bar*, 18 μm. *B*, determination of mean red:green fluorescence ratio in acridine orange-stained cells using flow cytometry. The mean red:green fluorescence ratio in irradiated and control unirradiated cells was determined as described in "Materials and Methods." *a* and *c*, unirradiated cells; *b* and *d*, 24 h after irradiation with 10 Gy; *c* and *d*, unirradiated and irradiated cells preincubated with 500 nM bafilomycin A1 30 min before the addition of acridine orange.

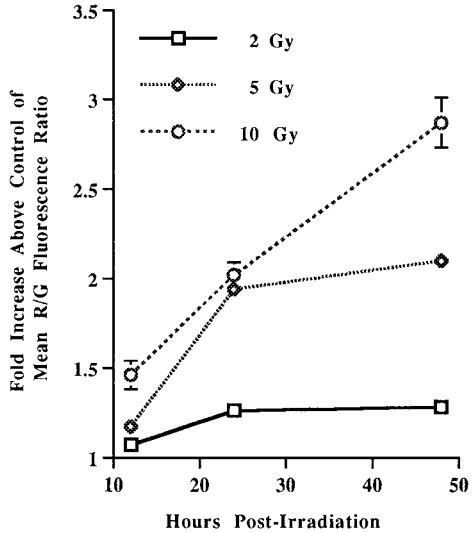

Fig. 4. Increased red:green (*R/G*) fluorescence ratio in irradiated cells is radiation dose- and time-dependent. Cells were stained and processed for flow cytometric analysis. The numbers represent the fold increase of the red:green fluorescence ratio in irradiated cells above controls, and are the mean ± SD of triplicate samples from one experiment that was reproduced twice with similar results.

The increase in the red:green fluorescence ratio could be modulated by PMA. The mean red:green fluorescence ratio increased by a factor of 1.7 ± 0.3 (n = 3) 48 h after stimulation with 30 nM PMA. This result suggests that protein kinase C may be involved in the increased red:green fluorescence ratio after irradiation.

The increase in the mean red:green fluorescence ratio after irradiation was also observed in two other cancer cell lines. Forty-eight h after irradiation with 10 Gy, the mean red:green fluorescence ratio increased in prostate cancer (LNCaP) and in colon adenocarcinoma (LoVo) cells by 1.6 ± 0.1 (n = 3) and 2 ± 0.2 (n = 3) -fold, respectively. As in MCF-7 cells, the increase in the mean red:green fluorescence ratio in LoVo and LNCaP cells was associated with the appearance of red fluorescent AVO.

Parallel investigations with electron microscopy confirmed the radiation-induced formation of a new acidic compartment (Fig. 2, *A* and *B*). These subcellular AVO were composed of core vesicles with granular, vesicular, or lamellar content. The core vesicles were often surrounded by and intertwined with smooth or part smooth/part rough membrane cisternae that were found to fuse with smooth vesicles of unknown origin (Fig. 2*B*). The diameter of these organelles ranged from 0.5–2.5 μm and was comparable with the diameter of the largest red fluorescent AVO in irradiated cells. Because fluorescent AVO may consist of a heterogeneous population of AVO, we termed the ones characterized by electron microscopy "AVO-EM." AVO-EM were found to be acidic by virtue of their ability to concentrate the lysosomotropic agent DAMP (Fig. 2*C*). By 48 h postirradiation with 10 Gy, the average fractional volume of AVO-EM in the population was 16 ± 0.1% (Fig. 2*D*), whereas, the average fractional volume in unirradiated cells was 0.91 ± 0.01%. The emergence of AVO-EM during the first 48 h postirradiation with 2–10 Gy was dose- and time-dependent (data not shown).

During autophagy, portions of the cytoplasm and subcellular organelles are sequestered by the endoplasmic reticulum, resulting in vesicular bodies that are bound by double-membrane cisternae (25). The association of the core vesicles with membrane cisternae in AVO-EM bears morphological similarities to autophagous bodies. We therefore examined the effect of 3-methyladenine, an inhibitor of autophagy (25, 26), on AVO formation. 3-Methyladenine at a final concentration of 5 mM decreased the red:green ratio at 48 h postradiation with 10 Gy from 1.77 ± 0.01 to 1.15 ± 0.01 (n = 3). Electron microscopy analysis demonstrated a parallel reduction in the fraction of cells containing AVO-EM from 94% to 22%. The effect of 3-methyladenine on irradiated cells suggests that the formation of AVO after irradiation may share similar pathways with processes that regulate autophagy.

It is important to note that in addition to ionizing irradiation, other death-inducing agents such as tumor necrosis factor and staurosporin kill MCF-7 without producing typical apoptotic changes (27). It has recently been reported that the lack of apoptotic response to tumor necrosis factor results from the absence of caspase-3 in these cells (27). The absence of caspase-3 may well explain the lack of apoptotic response to ionizing irradiation. Nonetheless, the emergence of AVO

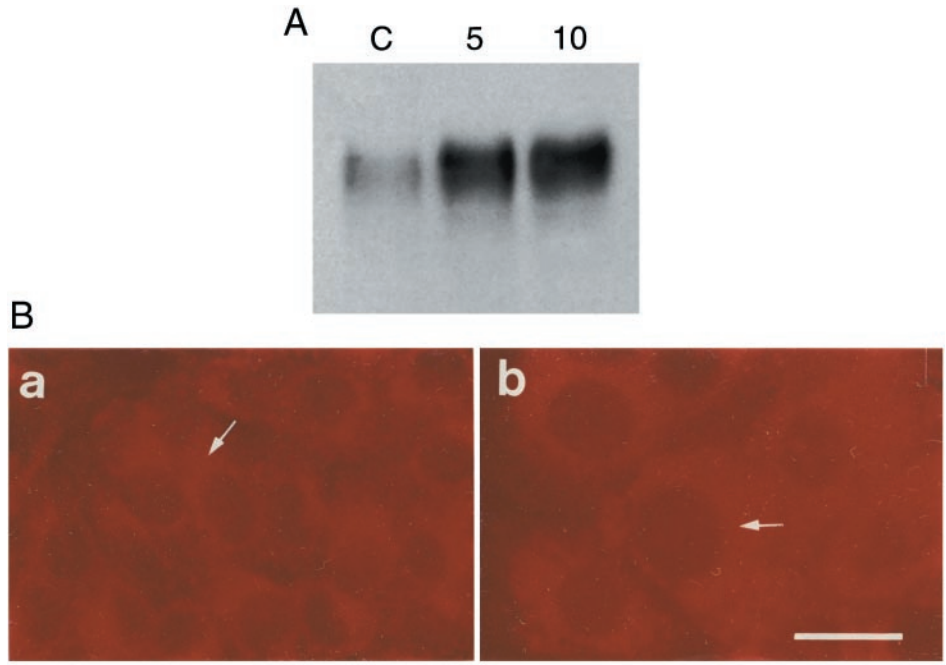

Fig. 5. Radiation induces increase in LAMP-1 levels. *A*, Western blotting analysis of LAMP-1. Cells were harvested 48 h after irradiation with 10 Gy. Equal amounts of cell lysates from control and irradiated cells were analyzed for LAMP-1 content. *C*, control unirradiated cells. *5*, cells irradiated with 5 Gy. *10*, Cells irradiated with 10 Gy. *B*, immunolocalization of LAMP-1 in control and irradiated cells. The staining showed the increased levels of LAMP-1 in the cells at 48 h after irradiation and its localization to vesicular bodies. *a*, unirradiated cells. *b*, cells irradiated with 10 Gy.

in the presence of the pan-caspase inhibitor z-VAD-fmk at concentrations ranging from 50–154 μM (Table 1) suggests that the programmed events that lead to AVO formation are not related to apoptosis.

Cells that survive radiation may continue to divide and form colonies, although their DNA might have sustained damage (28). We found that the progenies of irradiated cells contain an increased level of AVO (Table 2). This led us to postulate that the emergence of acidic compartments protects the cells against radiation damage. In fact, experiments with bafilomycin A1 showed that inhibition of vacuolar H^+-ATPase, the enzyme that mediates AVO acidification, augmented DNA degradation and decreased survival after irradiation (Fig. 6; Table 2). Addition of bafilomycin A1 2 days after irradiation with 10 Gy, for a period of 24 h, dramatically increased DNA cleavage into large fragments (20–1000 kb). Also, addition of bafilomycin A1 for 24 h after irradiation with 2 and 3 Gy reduced the surviving fraction by 30–40% without significantly affecting the survival of unirradiated cells.

Increased autophagy, the hallmark of programmed cell death type II, is thought to lead to cell death via destruction of the cytoplasm. Still, the lysosomal compartment has been linked to cellular defense mechanisms such as protection against infectious agents (29). Recently, acidic compartments have been associated with drug resistance of breast cancer cell lines (30), and in yeast autophagy is required for cell survival during starvation (31). Similarly, our results suggest that accumulation of AVO after irradiation is modulated by cellular defense mechanisms. These AVO may protect the cells by preventing cytoplasmic acidification, by providing catabolites required for repair processes, and/or by containing toxic molecules. Our experiments show that moderate formation of AVO in surviving colonies provides long-term protection against low-radiation damage. However, continuous accretion of AVO after high levels of damage may offset their protective effect, leading to replacement of the normal cytoplasm and possibly to necrosis and cell death. Therefore, inhibition of AVO formation or function may serve as a tool to increase cell death after low-radiation damage and facilitate cell-kill after high-radiation damage. Modulation of AVO function may prove useful for increasing the therapeutic ratio of radiation treatment of epithelial cancers.

Table 1 *Caspases do not mediate AVO formation*

z-VAD-fmk (Enzyme Systems Products, Livermore, CA) was added to cells 1 h before irradiation. Cells were harvested 24 h after irradiation and processed for determination of their mean red:green fluorescence ratio. Numbers are means ± SD from triplicate samples of one experiment that was reproduced twice at 50 μM and 154 μM.

z-VAD-fmk (50 μM)	−	+
Unirradiated	1.2 ± 0.05	1.4 ± 0.07
10 Gy	2.3 ± 0.08	2.5 ± 0.04

Table 2 *AVO accumulation in progenies of irradiated cells is necessary for their survival*

Red:green ratio in colonies was determined as described in "Materials and Methods." The numbers are mean ± SD from three separate experiments. Bafilomycin A1 was added to irradiated cells at the time of irradiation for 24 h. The effect of bafilomycin on the survival of irradiated cells was significant ($P < .05$; Student's t test). The numbers are mean ± SD from one experiment that was reproduced once with similar results. Colonies in five plates were counted for each dose.

Radiation dose (Gy)	Fold increase of mean R/G[a]	Surviving fraction	Surviving fraction in the presence of Baf A1[b] (2 nM)
0	1	1 ± 0.04	0.9 ± 0.14
2	1.2 ± 0.01	0.7 ± 0.09	0.51 ± 0.07
3	1.3 ± 0.1	0.42 ± 0.06	0.23 ± 0.05

[a] R/G, red:green ratio.
[b] Baf A1, bafilomycin A1.

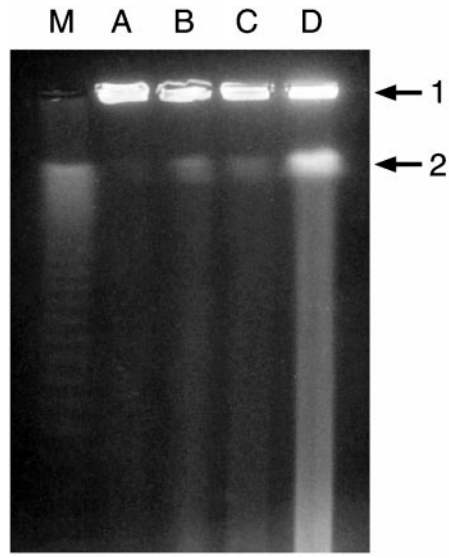

Fig. 6. Bafilomycin A1 enhances DNA fragmentation in irradiated cells. Cells were irradiated 48 h post-plating, and bafilomycin A1 (4 nM) was added 48 h after irradiation, for the duration of 24 h, from concentrated stock solution in DMSO to a final concentration of 4 nM. Control cells received the vehicle alone. Cells were harvested 72 h after irradiation. Plug preparation and resolution of DNA was conducted according to Gilles *et al.* (19) *M*, DNA size standard, lambda ladder (50 kb). *A*, unirradiated controls. *B*, cells irradiated with 10 Gy. *C*, unirradiated cells incubated with 4 nM bafilomycin A1. *D*, cells irradiated with 10 Gy and incubated with 4 nM bafilomycin A1. Window of DNA resolution was 20 kb–1000 kb. *Arrow 1* points to sample origin. *Arrow 2* points to zone of no resolution.

Acknowledgments

We thank Drs. David Golde, Haya Herscovitz, and Victoria Iwanij for critical reading of the manuscript; John Takawa from the Molecular Cytology Core Facility at the Memorial Sloan-Kettering Cancer Center for his help with the morphometric quantifications; Drs. Fred Gilles and Andre Goy for their help with the pulse field gel electrophoresis; and Vincent Yeugelowitz for excellent technical assistance.

References

1. Bristow, R. G., Benchimol, S., and Hill, R. P. The *p53* gene as a modifier of intrinsic radiosensitivity: implications for radiotherapy. Radiother. Oncol., *40:* 197–223, 1996.
2. Brown, M., and Wouters, B. G. Apoptosis, p53, and tumor cell sensitivity to anticancer agents. Cancer Res., *59:* 1391–1399, 1999.
3. Finkel, E. Does cancer therapy trigger cell suicide? Science (Washington DC), *286:* 2256–2258, 1999.
4. Schwartz, L. M., Smith, S. W., Jones, M. E. E., and Osborne, B. A. Do all programmed cell deaths occur via apoptosis? Proc. Natl. Acad. Sci. USA, *90:* 980–984, 1993.
5. Zakeri, Z., Bursch, W., Tenniswood, M., and Lockshin, R. A. Cell death: programmed apoptosis, necrosis, or other? Cell Death Differ., *2:* 87–96, 1995.
6. Reed, J. Dysregulation of apoptosis in cancer. J. Clin. Oncol., *17:* 2941–2953, 1999.
7. Bursch, W., Ellinger, A., Kienzl, H., Torok, L., Pandey, S., Sikovska, M., Walker, R., and Hermann, R. S. Active cell death induced by the anti-estrogens tamoxifen and ICI 164 384 in human mammary carcinoma cells (MCF-7) in culture: the role of autophagy. Carcinogenesis (Lond.), *17:* 1595–1607, 1996.
8. Jia, L., Dourmashkin, R. R., Allen, P. D., Gray, A. B., Newland, A. C., and Kelsey, S. M. Inhibition of autophagy abrogates tumour necrosis factor α-induced apoptosis in human T-lymphoblastic leukaemic cells. Br. J. Haematol., *98:* 673–685, 1997.
9. Paglin, S., Delohery, T., Erlandson, R., and Yahalom, J. Radiation-induced micronuclei formation in human breast cancer cells: dependence on serum and cell cycle distribution. Biochem. Biophys. Res. Commun., *237:* 678–684, 1997.
10. Haimovitz-Friedman, A., Kan, C., Ehleiter, D., Persaud, R., McLoughlin, M., Fuks, Z., and Kolesnik, R. Ionizing radiation acts on cellular membranes to generate ceramide and initiate apoptosis. J. Exp. Med., *180:* 525–535, 1994.
11. Verhij, M., Bose, R., Lin, X., Yao, B., Jarvis, W., Grant, S., Birrer, M., Haimovitz-Friedman, A., Fuks, Z., and Kolesnick, R. Requirement for ceramide-initiated SAPK/JNK signalling in stress-induced apoptosis. Nature (Lond.), *380:* 75–79, 1996.
12. Arvan, P., Rudnick, G., and Castle, J. D. Osmotic properties and internal pH of isolated rat parotid secretory granules. J. Biol. Chem., *259:* 13567–13572, 1984.

13. Mains, R. E., and May, V. The role of a low pH intracellular compartment in the processing, storage, and secretion of ACTH and endorphin. J. Biol. Chem., *263:* 7887–7894, 1988.
14. Traganos, F., and Darzynkiewicz, Z. Lysosomal proton pump activity: supravital cell staining with acridine orange differentiates leukocytes subpopulations. Vol. 41, pp. 185–194. New York: Academic Press, 1994.
15. Anderson, R. G. W., Falck, J. R., Goldstein, J. L., and Brown, M. S. Visualization of acidic organelles in intact cells by electron microscopy. Proc. Natl. Acad. Sci. USA, *81:* 4838–4842, 1984.
16. Dunn, W. A. Studies on the mechanisms of autophagy: maturation of the autophagic vacuole. J. Cell Biol., *110:* 1935–1945, 1990.
17. Lenk, S. E., Dunn, W. A., Trausch, J. S., Ciechanovev, A., and Schwarz, A. L. Ubiquitin-activating enzyme, E1, is associated with maturation of autophagic vacuoles. J. Cell Biol., *118:* 301–308, 1992.
18. Bose, R., Verheij, M., Haimovitz-Friedman, A., Scotto, K., Fuks, Z., and Kolesnick, R. Ceramide synthase mediates Daunorubicin-induced apoptosis: an alternative mechanism for generating death signals. Cell, *82:* 405–414, 1995.
19. Gilles, F., Goy, A., Remanche, Y., Shue, P., and Zelenetz, A. MUC1 dysregulation as the consequence of a t(1;14)(q21;q32) translocation in an extranodal lymphoma. Blood, *95:* 2930–2936, 2000.
20. O'Farrell, P. High resolution two-dimensional electrophoresis of proteins. J. Biol. Chem., *250:* 4007–4021, 1975.
21. Hall, E. J., and Phill, D. Radiobioloy for the Radiologist, Ed. 4, pp. 29–43. Philadelphia: J. B. Lippincott Company, 1994.
22. Wollman, R., Yahalom, J., Maxy, J., Pinto, J., and Fuks, Z. Effect of epidermal growth factor on the growth and radiation sensitivity of human breast cancer cells *in vitro*. Int. J. Radiat. Oncol. Biol. Phys., *30:* 91–98, 1994.
23. Bowman, E. J., Siebers, A., and Altendorf, K. Bafilomycins. A class of inhibitors of membrane ATPases from microorgansims, animal cells, and plant cells. Proc. Natl. Acad. Sci., *85:* 7972–7976, 1988.
24. Gagliardi, S., Rees, M., and Farina, C. Chemistry and structure activity relationships of bafilomycin A1, a potent and selective inhibitor of the vacuolar H+-ATPase. Curr. Med. Chem., *6:* 1197–1212, 1999.
25. Blommaart, E. F. C., Luiken, J. J. F. P., and Meijer, A. J. Autophagic proteolysis: control and specificity. Biochem. J., *29:* 365–385, 1997.
26. Seglen, P. O., and Gordon, P. B. 3-Methyladenine: specific inhibitor of autophagic/lysosomal protein degradation in isolated rat hepatocytes. Proc. Natl. Acad. Sci., USA, *79:* 1889–1892, 1982.
27. Janicke, R., Sprengart, M., Wati, M., and Porer, A. Caspase-3 is required for DNA fragmentation and morphological changes associated with apoptosis. J. Biol. Chem., *273:* 9357–9360, 1998.
28. Revell, S. H. Relationships between Chromosome Damage and Cell Death, Vol. 4, *In* T. Ishihara and M. S. Susaki (eds): Induced Chromosome Damage in Man, pp. 215–233. New York: Alan R. Liss, Inc., 1983.
29. Steinman, R., and Moberg, C. Zanvil Alexander Cohn 1926–1993. J. Exp. Med., *179:* 1–30, 1994.
30. Altan, N., Chen, Y., Schindler, M., and Simon, S. M. Defective acidification in human breast tumor cells and implications for chemotherapy., J. Exp. Med., *187:* 1583–1598, 1998.
31. Mizushima, N., Noda, T., Tamotsu, Y., Tanaka, Y., Ishii, T., George, M. D., Klionsky, D. J., Ohsumi, M., and Ohsumi, Y. A protein conjugation system essential for autophagy. Nature (Lond.), *395:* 395–398, 1998.

A Novel Response of Cancer Cells to Radiation Involves Autophagy and Formation of Acidic Vesicles

Shoshana Paglin, Timothy Hollister, Thomas Delohery, et al.

Cancer Res 2001;61:439-444.